PROCEEDINGS OF SCIENCE

Constraints on Intrinsic Charm from the SeaQuest Experiment

R. Vogt*

Nuclear and Chemical Sciences Division,
Lawrence Livermore National Laboratory, Livermore, CA 94551, USA
Department of Physics and Astronomy,
University of California, Davis, CA 95616, USA

E-mail: vogt2@llnl.gov

A nonperturbative charm production contribution, known as intrinsic charm, has long been speculated but has never been satisfactorily proven. The SeaQuest experiment at FNAL is in an ideal kinematic region to provide evidence of J/ψ production by intrinsic charm. Here, J/ψ production in the SeaQuest kinematics is calculated with a combination of perturbative QCD and intrinsic charm to see whether the SeaQuest data can put limits on an intrinsic charm contribution. J/ψ production in perturbative QCD is calculated to next-to-leading order in the cross section. Cold nuclear matter effects included in this component are nuclear modification of the parton densities, absorption by nucleons, and p_T broadening by multiple scattering. The J/ψ contribution from intrinsic charm is calculated assuming production from a $|uudc\overline{c}\rangle$ Fock state. The nuclear modification factor, R_{pA}, is calculated as a function of x_F and p_T for p+C, p+Fe, and p+W interactions relative to p + d. It is shown that the SeaQuest kinematic acceptance is ideal for setting limits on intrinsic charm in the proton.

**** 10th International Workshop on Charm Physics (CHARM2020), ****
**** 31 May - 4 June, 2021 ****
**** Mexico City, Mexico - Online ****

*Speaker

PoS(CHARM2020)038

1. Introduction

The production of J/ψ has been studied in a variety of environments, from $p+p$ and $p+\overline{p}$, to $p+A$, and $A+A$ collisions. In the last several years, J/ψ production has been studied by the SeaQuest experiment at Fermilab [1] in a fixed-target setup and at a lower incident proton energy than previous experiments, allowing unprecedented forward coverage probing partons carrying a large fraction, x_1, of the incident proton momentum.

Large x_1 coverage is ideal for setting limits on a $c\overline{c}$ component of the proton wavefunction, proposed by Brodsky and collaborators [2–4]. There have been some tantalizing hints, see the reviews in Refs. [5, 6] and the references therein, but no concrete confirmation so far. Fixed-target data either do not cover the far forward x_F region or have not had sufficient statistics to make a definitive statement. Production at collider energies usually pushes large x projectile partons outside the detector coverage [7]. Several additional new fixed-target experiments have been proposed [8, 9] or have taken data [10], including using the LHC for fixed-target studies [9, 10], but all are higher energy than SeaQuest.

The SeaQuest experiment at FNAL, with a 120 GeV incident proton beam, is in an ideal kinematic regime to test intrinsic charm production. Its J/ψ acceptance is in the region $0.4 < x_F < 0.95$ and $p_T < 2.3$ GeV. They have measured the x_F and p_T dependence of J/ψ production in $p+p$, $p+$d, $p+$C, $p+$Fe and $p+$W interactions [11].

The analysis of NA3 Collaboration [12] divided J/ψ production into two components that they referred to as hard and diffractive for the nuclear volume-like and surface-like dependencies,

$$\sigma_{pA} = A^{\alpha'}\sigma_h + A^{\beta}\sigma_d \ . \tag{1}$$

The hard component is calculated in perturbative QCD while the diffractive component has been attributed to intrinsic charm [2–4, 13]. Since the charm quark mass is large, these intrinsic heavy quark pairs carry a significant fraction of the longitudinal momentum and contribute at large x_F whereas perturbative charm production decreases strongly with x_F. The NA3 Collaboration found $\alpha' = 0.97$ and $\beta = 0.71$ for proton projectiles [12].

A similar two-component model is employed to make predictions for these measurements, at energies and with kinematic acceptance favorable to intrinsic charm, in this work. The results are expressed through the nuclear modification, R_{pA}, factor, the ratio of the per nucleon cross section in $p+A$ collisions relative to $p+$d interactions at the same energy, instead of α, as previously employed.

The calculation of J/ψ production in perturbative QCD is given in Sec. 2 and the cold nuclear matter effects included are introduced. The intrinsic charm contribution is described in Sec. 3, along with its nuclear dependence. Section 4 presents the results for the modification of J/ψ production in nuclear targets at SeaQuest. The conclusions are presented in Sec. 5.

2. J/ψ Production and Cold Nuclear Matter Effects in Perturbative QCD

Here, J/ψ production in perturbative QCD is discussed and the implementation of cold nuclear matter effects in this work is described. The Color Evaporation Model [14] is employed. This model, together with the Improved Color Evaporation Model [15], can describe the x_F and p_T distributions

of J/ψ production, including at low p_T. The cold nuclear matter effects included in the CEM are: nuclear modifications of the parton densities, nPDF effects; absorption by nucleons; and transverse momentum broadening. This contribution is the hard part of the cross section, σ_h, in Eq. (1).

The Color Evaporation Model [14] assumes that a fraction, F_C, of the $c\overline{c}$ pairs produced in perturbative QCD with a pair mass below twice the D meson mass will go on mass shell as a J/ψ,

$$\sigma_{\rm CEM}(pp) = F_C \sum_{i,j} \int_{4m^2}^{4m_H^2} ds \int dx_1\, dx_2\, F_i^p(x_1,\mu_F^2,k_{T_1})\, F_j^p(x_2,\mu_F^2,k_{T_2})\, \hat{\sigma}_{ij}(\hat{s},\mu_F^2,\mu_R^2)\ , \quad (2)$$

where $ij = gg, q\overline{q}$ or $q(\overline{q})g$ and $\hat{\sigma}_{ij}(\hat{s},\mu_F^2,\mu_R^2)$ is the partonic cross section for initial state ij evaluated at factorization scale μ_F and renormalization scale μ_R. The parton densities are written to include intrinsic k_T, required to keep the pair cross section finite as $p_T \to 0$. They are assumed to factorize into the longitudinal, collinear parton densities and a k_T-dependent function, $F^p(x,\mu_F^2,k_T) = f^p(x,\mu_F^2)G_p(k_T)$. The CT10 proton parton densities [16] are used for $f^p(x,\mu_F^2)$. The values of charm quark mass, m, and scales μ_F and μ_R determined in Ref. [17] are employed.

Calculations in the CEM were carried out at next-to-leading order (NLO) in the heavy flavor cross section using the exclusive NLO $Q\overline{Q}$ production code HVQMNR [18] after imposing a cut on the pair invariant mass. To keep the p_T distribution finite as $p_T \to 0$, the calculations require augmentation by k_T broadening. An intrinsic k_T is added in the final state. Because the kick is employed in the final state the factors $G_p(k_T)$ are replaced by $g_p(k_T) = G_p(k_{T_1})G_p(k_{T_2})$ where $g_p(k_T)$ is a Gaussian [19], $g_p(k_T) = \frac{1}{\pi\langle k_T^2\rangle_p}\exp(-k_T^2/\langle k_T^2\rangle_p)$.

The value of $\langle k_T^2\rangle_p$ is assumed to increase with $\sqrt{s}$ [17],

$$\langle k_T^2\rangle_p = \left[1 + \frac{1}{n}\ln\left(\frac{\sqrt{s_{NN}}({\rm GeV})}{20\,{\rm GeV}}\right)\right]\ {\rm GeV}^2 \quad (3)$$

with $n = 12$ [17]. At the SeaQuest energy, $\sqrt{s_{NN}} = 15.4$ GeV, $\langle k_T^2\rangle_p = 0.97$ GeV^2.

Nuclear parton densities (nPDFs) are implemented employing a parameterization of the modification in the nucleus as a function of x, μ_F and A, The k_T-independent proton parton distribution function in Eq. (2) is replaced by the nuclear parton distribution function $f_j^A(x_2,\mu_F^2) = R_j(x_2,\mu_F^2,A)f_j^p(x_2,\mu_F^2)$. The EPPS16 [20] nPDF parameterization is employed in the calculations. It is available for $A = 12$ (carbon), 56 (iron) and 184 (tungsten) but assumes no modification for the deuteron target. The SeaQuest acceptance probes the range $0.068 < x_2 < 0.136$.

The effect of nuclear absorption alone on the J/ψ production cross section in $p+A$ collisions is implemented as a survival probability as a function of impact parameter, $S^{\rm abs}(b) \sim \exp(-L\rho_A\sigma_{\rm abs})$ where L is the path length through the nucleus, ρ_A is the nuclear density and $\sigma_{\rm abs}$ is the J/ψ absorption cross section. The extracted absorption cross section also depends on which cold nuclear matter effects are taken into account. An energy-dependent effective absorption cross section was obtained in Ref. [21]. A value of $\sigma^{\rm abs} = 9$ mb is found by extrapolating the results from Ref. [21] to the SeaQuest energy.

The intrinsic k_T broadening employed in the J/ψ p_T distribution in $p+p$ collisions in Eq. (3) is augmented in a nuclear target due to multiple scattering in the nucleus [22]. It is implemented

by replacing $g_p(k_T)$ by $g_A(k_T)$ with $\langle k_T\rangle_p$ replaced by $\langle k_T\rangle_A$ where [23]

$$\langle k_T^2\rangle_A = \langle k_T^2\rangle_p + \delta k_T^2 \ , \tag{4}$$

$$\delta k_T^2 \approx (0.92A^{1/3} - 1) \times 0.101 \ \mathrm{GeV}^2 \ . \tag{5}$$

For carbon, iron and tungsten targets, $\delta k_T^2 = 0.1$, 0.25, and 0.39 GeV^2 respectively, resulting in an average broadening in the nucleus of $\langle k_T^2\rangle_A = 1.07$, 1.22, and 1.36 GeV^2 for the SeaQuest targets.

3. Intrinsic Charm

The wave function of a proton in QCD can be represented as a superposition of Fock state fluctuations, *e.g.* $|uudg\rangle$, $|uudq\overline{q}\rangle$, $|uudQ\overline{Q}\rangle$, ... of the $|uud\rangle$ state. These intrinsic $Q\overline{Q}$ Fock states are dominated by configurations with equal rapidity constituents so that the intrinsic heavy quarks carry a large fraction of the projectile momentum [2, 3].

The probability distribution of a 5-particle $c\overline{c}$ Fock state in the proton is

$$dP_{\mathrm{ic}\,5} = P^0_{\mathrm{ic}\,5} N_5 \int \prod_{i=1}^{5} dx_i dk_{x\,i} dk_{y\,i} \frac{\delta(1-\sum_{i=1}^5 x_i)\delta(\sum_{i=1}^5 k_{x\,i})\delta(\sum_{i=1}^5 k_{y\,i})}{(m_p^2 - \sum_{i=1}^5 (\widehat{m}_i^2/x_i))^2} \ , \tag{6}$$

where i = 1, 2, 3 represent the light quarks (u, u, d) and i = 4 and 5 are the c and $\overline{c}$ quarks respectively. The factor N_5 normalizes the $|uudc\overline{c}\rangle$ probability to unity and $P^0_{\mathrm{ic}\,5}$ scales the unit-normalized probability to the assumed intrinsic charm content of the proton. Several values of the intrinsic charm probability, $P^0_{\mathrm{ic}\,5}$, are employed. The EMC charm structure function data is consistent with $P^0_{\mathrm{ic}\,5} = 0.31\%$ for low energy virtual photons but $P^0_{\mathrm{ic}\,5}$ could be as large as 1% for the highest virtual photon energies [24, 25]. For a lower limit, a probability of 0.1% is used.

The delta functions in Eq. (6) conserve longitudinal and transverse momentum. Previously only the x_F dependence of the J/ψ from the 5-particle Fock state was considered, employing average values for the transverse masses, $\widehat{m}_i^2 = m_i^2 + k_{T\,i}^2$, with $\widehat{m}_q = 0.45$ GeV and $\widehat{m}_c = 1.8$ GeV [13]. Then the J/ψ x_F distribution can be calculated assuming coalescence of the c and $\overline{c}$ in Eq. (6) by including $\delta(x_F - x_c - x_{\overline{c}}$ for the longitudinal momentum. The p_T distribution of the J/ψ from this Fock state was calculated for the first time in Ref. [23], assuming the J/ψ p_T is only in the x direction, introducing two additional delta functions in Eq. (6): $\delta(p_T - k_{x\,c} - k_{x\,\overline{c}})$ and $\delta(k_{y\,c} + k_{y\,\overline{c}})$.

While the x_F dependence is independent of the k_T limits, the p_T distributions depend significantly on the range of k_T integration. The chosen default values are $k_q^{\mathrm{max}} = 0.2$ GeV and $k_c^{\mathrm{max}} = 1.0$ GeV. If the limits of the integration range are doubled to $k_q^{\mathrm{max}} = 0.4$ GeV and $k_c^{\mathrm{max}} = 2.0$ GeV, the p_T distribution becomes broader. On the other hand, halving the integration range to 0.1 GeV and 0.5 GeV for the light and charm quarks makes the distribution steeper.

It is worth noting that the J/ψ p_T distribution from intrinsic charm is considerably broader than that of the J/ψ calculated with the CEM. In perturbative QCD, the p_T range depends on the center of mass energy with a limit of $m_T \sim \sqrt{s_{NN}}/2$ at $x_F = 0$ for massive quarks. Assuming $2 \to 2$ scattering, the maximum J/ψ p_T is $p_T \le 6.5$ GeV in the CEM. In addition, since the initial light partons that create the $c\overline{c}$ that becomes a J/ψ come from both the projectile and the target, one will carry a much smaller fraction of the hadron momentum that the intrinsic charm quarks in the proton $|uudc\overline{c}\rangle$ Fock state. On the other hand, when the J/ψ arises from an intrinsic charm state of

the proton, there is no energy limit on the J/ψ p_T distribution other than momentum conservation. The J/ψ kinematics all come from the incident proton. Only a soft interaction with the target is sufficient to disrupt the Fock state and bring the J/ψ on mass shell.

It is important to properly normalize the intrinsic charm contribution to the J/ψ cross section to put the two components of the cross section on the same footing. The intrinsic charm production cross section from the $|uudc\overline{c}\rangle$ component of the proton can be written as

$$\sigma_{\rm ic}(pp) = P_{\rm ic\,5}\sigma_{pN}^{\rm in}\frac{\mu^2}{4\widehat{m}_c^2} \ . \tag{7}$$

The factor of $\mu^2/4\widehat{m}_c^2$ arises from the soft interaction which breaks the coherence of the Fock state where $\mu^2 = 0.1$ GeV^2 is assumed, see Ref. [13], and $\sigma_{pN}^{\rm in} = 30$ mb is appropriate for the SeaQuest energy. The J/ψ contribution is obtained by scaling Eq. (7) by the same factor, F_C, used to scale the CEM calculation to obtain the inclusive J/ψ cross section from the $c\overline{c}$ cross section in Eq. (2),

$$\sigma_{\rm ic}^{J/\psi}(pp) = F_C\sigma_{\rm ic}(pp) \ . \tag{8}$$

4. Results

The nuclear suppression factor,

$$R_{pA} = \frac{2}{A}\frac{\sigma_{pA}}{\sigma_{p\rm d}} \ , \tag{9}$$

is calculated for the J/ψ in the SeaQuest kinematics. In Eq. (9) the cross section per nucleon in a nuclear target is compared to that of the deuteron target. The relative per nucleon cross sections are a more straightforward way to present the nuclear dependence than averaging over all targets by employing the exponent α, as was done previously. Note that using the deuteron target as the baseline for the suppression factor reduces the potential, albeit small, isospin dependence of the ratios. The individual cross sections in the suppression factor are

$$\sigma_{pA} = \sigma_{\rm CEM}(pA) + \sigma_{\rm ic}^{J/\psi}(pA) \tag{10}$$

$$\sigma_{p\rm d} = 2\sigma_{\rm CEM}(pp) + \sigma_{\rm ic}^{J/\psi}(pA) \ . \tag{11}$$

The A dependence of the CEM contribution to the cross section is

$$\sigma_{\rm CEM}(pA) = S_A^{\rm abs}F_C\sum_{i,j}\int_{4m^2}^{4m_H^2} ds \int dx_1\,dx_2\ F_i^p(x_1,\mu_F^2,k_T)\ F_j^A(x_2,\mu_F^2,k_T)\ \hat{\sigma}_{ij}(\hat{s},\mu_F^2,\mu_R^2) \ , \tag{12}$$

where

$$F_j^A(x_2,\mu_F^2,k_T) = R_j(x_2,\mu_F^2,A)f_j(x_2,\mu_F^2)G_A(k_T) \tag{13}$$

$$F_i^p(x_1,\mu_F^2,k_T) = f_i(x_1,\mu_F^2)G_p(k_T) \ . \tag{14}$$

The k_T broadening is $g_A(k_T) = G_p(k_{T_1})G_A(k_{T_2})$. where, in the nuclear target, $\langle k_T^2\rangle_A^{1/2}$ from Eq. (4) is used. In the case of the deuteron target, $R_j \equiv 1$ in EPPS16, and $\delta k_T^2 = 0$ in Eq. (5) so that $g_A(k_T) = g_p(k_T)$. It is also assumed that $\sigma_{\rm abs} = 0$ for the deuteron. Thus $\sigma_{p\rm d} = 2\sigma_{\rm CEM}(pp)$.

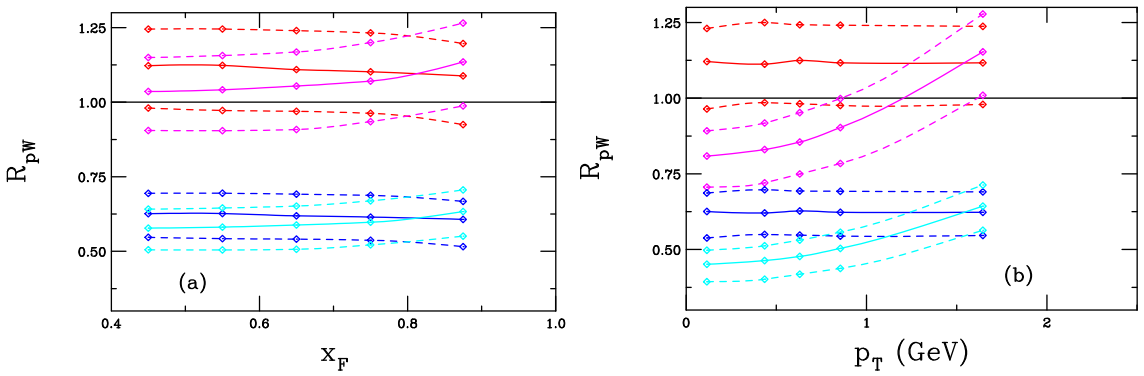

Figure 1: The nuclear modification factors for J/ψ production in SeaQuest as a function of x_F for pQCD production alone for a tungsten target relative to deuterium as a function of x_F (a) and p_T (b). Results are shown for nPDF effects alone (red), nPDFs with an additional k_T kick (magenta), nPDFs and absorption (blue), and nPDFs, absorption and k_T broadening (cyan). The solid lines shown the results with the central EPPS16 set while the dashed curves denote the limits of adding the EPPS16 uncertainties in quadrature.

The nuclear dependence of the intrinsic charm contribution is assumed to be the same as that extracted for the diffractive component of J/ψ production [12] in Eq. (1), so that

$$\sigma_{\rm ic}^{J/\psi}(pA) = \sigma_{\rm ic}^{J/\psi}(pp)\, A^{\beta} \tag{15}$$

with $\beta = 0.71$ [12] for a proton beam.

The calculations are all in the x_F and p_T bins defined by SeaQuest [11]. The calculated points shown in the figures are placed at the arithmetic center of the bin rather than a cross-section weighted center. Changing the location of the calculated points within the bins could slightly modify the shape of the x_F and p_T dependence but would not alter any conclusions. Because the SeaQuest data have not yet been submitted for publication, the calculations cannot yet be compared to data.

The results here are shown only for the tungsten target, $p+$W. Reference [23] shows the results for all SeaQuest targets as well as comparisons to the higher energy E866 [26] measurements of the nuclear dependence as a function of x_F and p_T in three different x_F bins. The effects are added sequentially in these figures. Only nPDF effects are common to all the calculated ratios. These nPDF results are presented with the central, best fit, set given by the solid curves while the uncertainties added in quadrature are outlined by the dashed curves.

First nPDF effects alone are shown in Fig. 1 by the red points and curves. In this case, $g_A(k_T) = g_p(k_T)$, no additional broadening is taken into account due to the nuclear target. The magenta points and curves show the effect of enhanced k_T broadening in the nuclear target. Next, absorption is added in the two cases with nPDF effects plus absorption shown in the blue points and curves while all three effects: nPDF, absorption and enhanced k_T broadening are shown by the cyan points and curves.

The results with nPDF effects alone are generally independent of x_F and p_T with $R_{pA} > 1$. The scale of the calculation, not much greater than the minimum scale of EPPS16, indicates that the uncertainties will be larger than at higher scales. The EPPS16 nPDF uncertainties are large.

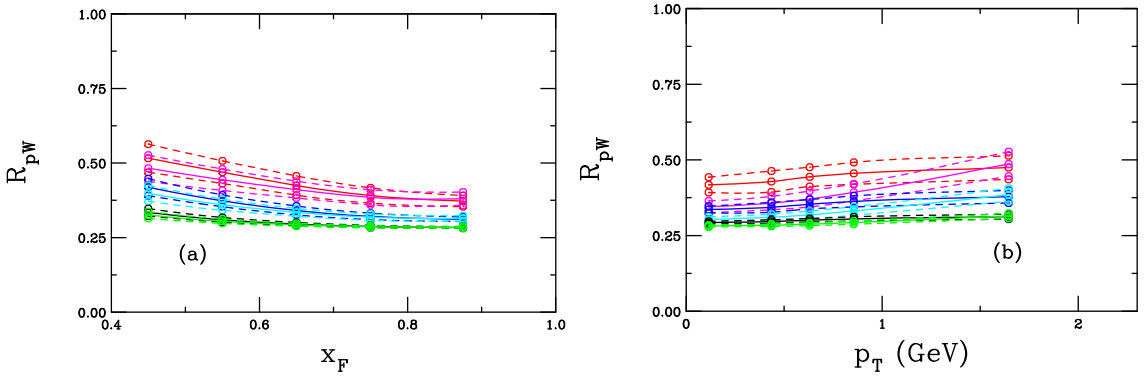

Figure 2: The nuclear modification factors for J/ψ production in SeaQuest as a function of x_F (a) and p_T (b) for the combined pQCD and intrinsic charm cross section ratios for tungsten targets relative to deuterium. All calculations are shown with nuclear absorption included. Results with EPPS16 and the same k_T in $p+\mathrm{d}$ and $p+A$ are shown in the red, blue and black curves while EPPS16 with an enhanced k_T kick in the nucleus are shown in the magenta, cyan and green curves. The probability for IC production is 0.1% in the red and magenta curves; 0.31% in the blue and cyan curves; and 1% in the black and green curves. The solid lines shown the results with the central EPPS16 set while the dashed curves denote the limits of adding the EPPS16 uncertainties in quadrature.

The effect of k_T broadening in the nucleus relative to the deuteron changes the shape of the p_T distribution, particularly at low p_T. Because the mass scale of the J/ψ is larger than the applied k_T kick, the low center of mass energy of the SeaQuest experiment results in a larger effect than at higher energies. This effect is particularly notable on $R_{pA}(p_T)$ in Fig. 1(b). The broadening results in a substantial increase in R_{pA} with p_T.

There is also a slight change in the x_F dependence of R_{pA} due to broadening since $x_F = 2m_T \sinh y/\sqrt{s_{NN}}$. This change is small because x_F depends on $m_T = \sqrt{m^2 + p_T^2}$ and m and p_T are of comparable magnitude over the measured p_T range.

Rather strong absorption is required to nullify the effects of antishadowing and produce $R_{pA} < 1$, as seen when absorption is added to the calculation. Since a constant 9 mb cross section has been assumed, as inferred for midrapidity ($x_F \sim 0$) in Ref. [21], absorption does not change the dependence of R_{pA} on x_F and p_T.

Intrinsic charm is now added to the calculations of R_{pA} in Fig. 2. Three values of $P^0_{\mathrm{ic}\,5}$ in Eq. (6) are shown in the following four figures: 0.1%, 0.31% and 1%. This range can be taken as an uncertainty band on intrinsic charm. The EPPS16 results are presented with the central set given by the solid curves while the uncertainties added in quadrature are shown by the dashed curves.

The red, blue and black curves show the nPDF effects with $P^0_{\mathrm{ic}\,5} = 0.1\%$, 0.31% and 1% respectively in Fig. 2. The solid curves show the EPPS16 central value while the dashed curves outline the uncertainty band. For these calculations, $g_A(k_T) = g_p(k_T)$. The magenta, cyan and green solid and dashed curves include enhanced k_T broadening in the nuclear target for $P^0_{\mathrm{ic}\,5} = 0.1\%$, 0.31% and 1% respectively.

Including intrinsic charm makes $R_{pA}(x_F)$ decrease with increasing x_F while it reduces the strong p_T dependence observed with k_T broadening shown in Fig. 1(b). The strong absorption

cross section employed in these calculations, $\sigma_{\rm abs}$ = 9 mb, results in dominance of the intrinsic charm contribution even when $P^0_{\rm ic\,5}$ is as low as 0.1%. The strong absorption compresses the pQCD uncertainties due to nPDF effects and k_T broadening. The differences between the calculations with nPDF effects only and nPDFs with k_T broadening are almost indistinguishable. If absorption is not included, there is an observable separation between the values of $P^0_{\rm ic\,5}$.

5. Conclusions

The low energy of the SeaQuest experiment, as well as its forward acceptance, makes it an ideal experiment to test the existence of an intrinsic charm contribution to J/ψ production. The energy, a factor of 3.1 above the J/ψ production threshold, means that the perturbative QCD cross section is of the same order as the J/ψ cross section from intrinsic charm.

Higher center of mass energies increase the J/ψ cross section in the CEM dramatically, see, *e.g.* Ref. [17], while the intrinsic charm contribution grows more slowly, depending only on $\sigma^{\rm in}_{pN}$, see Eq. (7). In addition, the high x_F range covered by SeaQuest is exactly the region where intrinsic charm should dominate production. Thus higher energies will reduce the potential for seeing an intrinsic charm signal, especially if the detector setups do not cover sufficiently high x_F. Fixed-target kinematics are thus preferable for the discovery potential of intrinsic charm.

A comparison of the SeaQuest J/ψ production data on its nuclear targets, once available, could set limits on $\sigma_{\rm abs}$ in the perturbative QCD contribution and $P^0_{\rm ic\,5}$, the probability of the intrinsic charm contribution in the proton.

Acknowledgments I thank C. Aidala, A. Angerami, C. Ayuso and V. Cheung for discussions. This work was supported by the Office of Nuclear Physics in the U.S. Department of Energy under Contract DE-AC52-07NA27344 and the LLNL-LDRD Program Project No. 21-LW-034.

References

[1] C. A. Aidala *et al.* [SeaQuest Collaboration], *The SeaQuest Spectrometer at Fermilab*, Nucl. Instrum. Meth. A **930**, 49 (2019).

[2] S. J. Brodsky, P. Hoyer, C. Peterson, and N. Sakai, *The Intrinsic Charm of the Proton*, Phys. Lett. B **93**, 451 (1980).

[3] S. J. Brodsky, C. Peterson, and N. Sakai, *Intrinsic Heavy Quark States*, Phys. Rev. D **23**, 2745 (1981).

[4] S. J. Brodsky and P. Hoyer, *The Nucleus as a Color Filter in QCD Decays: Hadroproduction in Nuclei*, Phys. Rev. Lett. **63**, 1566 (1989).

[5] S. J. Brodsky, A. Kusina, F. Lyonnet, I. Schienbein, H. Spiesberger, and R. Vogt, *A review of the intrinsic heavy quark content of the nucleon*, Adv. High Energy Phys. **2015**, 341547 (2015).

[6] S. J. Brodsky, G. I. Lykasov, A. V. Lipatov and J. Smiesko, *Novel Heavy-Quark Physics Phenomena*, Prog. Part. Nucl. Phys. **114**, 103802 (2020).

[7] R. Vogt and S. J. Brodsky, *Intrinsic charm production of doubly charmed baryons: Collider vs. fixed-target*, Sci. China Phys. Mech. Astron. **63**, 221066 (2020).

[8] M. Agnello *et al.* [NA60+ Collaboration], *Study of hard and electromagnetic processes at CERN-SPS energies: an investigation of the high-$\mu_{\mathbf{B}}$ region of the QCD phase diagram with NA60+*, [arXiv:1812.07948 [nucl-ex]].

[9] L. Massacrier, B. Trzeciak, F. Fleuret, C. Hadjidakis, D. Kikola, J. P. Lansberg and H. S. Shao, *Feasibility studies for quarkonium production at a fixed-target experiment using the LHC proton and lead beams (AFTER@LHC)*, Adv. High Energy Phys. **2015**, 986348 (2015).

[10] R. Aaij *et al.* [LHCb Collaboration], *First Measurement of Charm Production in its Fixed-Target Configuration at the LHC*, Phys. Rev. Lett. **122**, 132002 (2019).

[11] C. Ayuso, *Nuclear modification of J/ψ and Drell-Yan production at the E906/SeaQuest experiment*, doi:10.2172/1637630.

[12] J. Badier *et al.* [NA3 Collaboration], *Experimental J/ψ Hadronic Production from 150 GeV/c to 280 GeV/c*, Z. Phys. C **20**, 101 (1983).

[13] R. Vogt, S.J. Brodsky, and P. Hoyer, *Systematics of J/ψ Production*, Nucl. Phys. B **360** 67, (1991).

[14] R. Gavai, D. Kharzeev, H. Satz, G. A. Schuler, K. Sridhar and R. Vogt, *Quarkonium production in hadronic collisions*, Int. J. Mod. Phys. A **10**, 3043 (1995).

[15] Y. Q. Ma and R. Vogt, *Quarkonium Production in an Improved Color Evaporation Model*, Phys. Rev. D **94**, 114029 (2016).

[16] H. L. Lai, M. Guzzi, J. Huston, Z. Li, P. M. Nadolsky, J. Pumplin and C. P. Yuan, *New parton distributions for collider physics*, Phys. Rev. D **82**, 074024 (2010).

[17] R. E. Nelson, R. Vogt and A. D. Frawley, *Narrowing the uncertainty on the total charm cross section and its effect on the J/ψ cross section*, Phys. Rev. C **87**, 014908 (2013).

[18] M. L. Mangano, P. Nason, and G. Ridolfi, *Heavy quark correlations in hadron collisions at next-to-leading order*, Nucl. Phys. B **373**, 295 (1992).

[19] M. L. Mangano, P. Nason and G. Ridolfi, *Fixed target hadroproduction of heavy quarks*, Nucl. Phys. B **405**, 507 (1993).

[20] K. J. Eskola, P. Paakkinen, H. Paukkunen and C. A. Salgado, *EPPS16: Nuclear parton distributions with LHC data*, Eur. Phys. J. C **77**, 163 (2017).

[21] C. Lourenco, R. Vogt and H. K. Woehri, *Energy dependence of J/ψ absorption in proton-nucleus collisions*, JHEP **02**, 014 (2009).

[22] J. W. Cronin, H. J. Frisch, M. J. Shochet, J. P. Boymond, R. Mermod, P. A. Piroue and R. L. Sumner, *Production of hadrons with large transverse momentum at 200, 300, and 400 GeV*, Phys. Rev. D **11**, 3105 (1975).

[23] R. Vogt, *Limits on Intrinsic Charm Production from the SeaQuest Experiment*, Phys. Rev. C **103**, 035204 (2021).

[24] J. J. Aubert *et al.* [EMC Collaboration], *An Experimental Limit on the Intrinsic Charm Component of the Nucleon*, Phys. Lett. B **110**, 73 (1982).

[25] B. W. Harris, J. Smith, and R. Vogt, *Reanalysis of the EMC charm production data with extrinsic and intrinsic charm at NLO*, Nucl. Phys. B **461**, 181 (1996).

[26] M. J. Leitch, W. M. Lee, M. E. Beddo, C. N. Brown, T. A. Carey, T. H. Chang *et al.* [NuSea Collaboration], *Measurement of J/ψ and ψ' suppression in $p-A$ collisions at 800 GeV/c*, Phys. Rev. Lett. **84**, 3256 (2000).